DOE/NV/25946--512

Monte Carlo simulations of high-speed, time-gated MCP–based x-ray detectors: saturation effects in DC and pulsed modes and detector dynamic range[a]

Craig A. Kruschwitz, Ming Wu, and Ken Moy

National Security Technologies, LLC, Los Alamos, New Mexico 87544

Greg Rochau

Sandia National Laboratories, Albuquerque, New Mexico 87185

We present here results of continued efforts to understand the performance of microchannel plate (MCP)–based, high-speed, gated, x-ray detectors. This work involves the continued improvement of a Monte Carlo simulation code to describe MCP performance coupled with experimental efforts to better characterize such detectors. Our goal is a quantitative description of MCP saturation behavior in both static and pulsed modes. A new model of charge buildup on the walls of the MCP channels is briefly described. The simulation results agree favorably with experimental data obtained with a short-pulse, high-intensity ultraviolet (UV) laser. These results indicate that a weak

---

[a]Contributed paper, published as part of the Proceedings of the 17th Topical Conference on High-Temperature Plasma Diagnostics, Albuquerque, New Mexico, May 2008.

saturation can change the exponent of gain with voltage and that a strong saturation lead to a gain plateau. These results also demonstrate that the dynamic range of an MCP in pulsed mode has a value of between 10^2 and 10^3.

I. INTRODUCTION

High-speed, gated x-ray detectors based on straight-channel MCPs are a powerful diagnostic tool for two-dimensional, time-resolved imaging and time-resolved x-ray spectroscopy. Such detectors have become standard diagnostics on fast Z-pinch experiments and laser-driven inertial confinement fusion experiments. These detectors consist of an MCP, a phosphor screen coated on a fiber-optic faceplate, and a film recorder or charge-coupled device (CCD) camera to record the image. Detector gating is achieved by sending a subnanosecond high-voltage pulse through a microstrip transmission line coated onto the MCP. As the high-voltage pulse propagates along the strip line, MCP gating occurs wherever the voltage is applied.

In this paper we report on efforts to simulate, using Monte Carlo methods, the behavior and performance of MCP–based x-ray detectors. Specifically, we studied a newly designed 8-half frame MCP detector, which is similar to the detectors used in the multilayer mirror (MLM) pinhole camera diagnostic at the Sandia National Laboratories Z facility.[1] Several reengineering improvements in the new National Security Technologies (NSTec) camera increased significantly its reliability, sensitivity, and gain uniformity. In addition, extensive experimental efforts have been made to fully characterize the 8-frame camera, resulting in a large body of available experimental data. Much of this data was obtained using a subpicosecond, high-intensity UV laser (200-nm

wavelength), which was used to investigate MCP dynamic range and gain saturation. Understanding these MCP characteristics is essential in order to fully comprehend the experimental data obtained using the camera.

II. SIMULATION MODEL

The Monte Carlo model we used has been described by Wu *et al*.[2] in detail. Essentially, the code uses typical secondary electron emission probability distributions to describe the electron multiplication and cascade down a single channel in the MCP. The code is similar to those used by previous authors,[3,4,5,6] but contains a more detailed physical model of the cascade and amplification processes. The model is easily adaptable to MCPs with a broad range of parameters, but our primary interest has been with those used in the 8-frame camera, which have a pore length to diameter ratio (L/D ratio) of 46, and a pore diameter of 10 microns.

A simulation is begun by specifying a mean number of initial, or primary, electrons. The actual number of primary electrons is sampled from a Poisson distribution. The primary electrons are assumed to be generated by interactions of UV photons with the reduced lead glass channel surface near the MCP's input face. The simulation proceeds by calculating the trajectories of the primary electrons in the channel under the influence of the applied voltage. Each electron is determined to either collide with the channel wall or leave the channel. If a collision occurs then the primary either reflects or produces some number of secondary electrons according to the criteria described by Wu *et al*.,[2] thus continuing the cascade. The process continues until no further collisions occur and the cascade stops.

Our model can simulate MCP response to both static and pulsed voltage biases. Static voltage bias is simply handled, as the value of the voltage does not change over the duration of the electron cascade. We assume, following Gatti *et al*.,[7] that for static voltages the electric field is parallel to the channel axis. Time-dependence of the voltage pulse is approximated in the following way: when a secondary electron is created, the value of the voltage at the time of creation is determined and the electron's trajectory is calculated using that voltage. Since the typical electron time of flight is 5–10 ps, this approximation should be valid. For pulsed voltage biases we take the field to be perpendicular to the face of the MCP.[8]

As a result of the electron multiplication process there is a buildup of positive charge on the walls of the channel. The rate at which the lost electrons are replaced by the bias current is on the order of milliseconds,[9] much longer than the ~200 ps electron transit time, and so is unimportant for our simulations. The result of this charge buildup is the creation of a positive potential that increases the effective electron affinity. Secondary electrons with insufficient energy to overcome this increased affinity remain trapped within the glass. This effect has been studied in detail by Cazaux.[8,10] Although MCP glass was not studied, the effect should apply to electron generation in an MCP and was thus included in our simulations.

III. SHORT-PULSE UV LASER EXPERIMENTS

The characterization of MCP detectors was conducted at the Short-Pulse Laser Facility at NSTec Livermore Operations, which provided 200-nm laser light with a 150–200 fs pulse width at 150–200 μJ energy per pulse. The laser beam was expanded to

cover the entire MCP detector. Laser beam uniformity was achieved by a homogenizer and diffuser, and the laser flux was adjusted by a set of neutral density filters. Sensitivity and saturation effects of the MCP in DC mode were measured by varying the DC bias voltage and laser flux. MCP saturation in pulsed mode was studied by varying the laser flux when the laser pulse and high-voltage (HV) pulse overlapped at positions of interest. The timing jitter in the experiments was 25 ps or less.

For both static and pulsed bias experiments the phosphor was held by a 2-μs, +3000-V pulse with respect to the MCP back surface. A coherent fiber plug (38 mm high, 38 mm wide, and 140 mm long) was used to couple the phosphor and the CCD camera. The glass fibers were 4.5 μm in diameter, and the overall quality area was 35 × 38 mm. The CCD camera was a Spectral Instruments 800 series with a KAF-16801E class 2 chip with 4096H × 4096V (9-μm) photoactive pixels.

For the static bias voltage experiments, each of the eight strips on the MCP was held at the same voltage, which ran from –400 to –900 VDC in 50-V increments. The laser power was adjusted using the neutral density filters so that the experiment was performed over a two order of magnitude range of fluxes from ~10^4 to 10^6 photons/channel, allowing study of the MCP response to static voltages in saturated and unsaturated regimes. Average sensitivity was calculated as the average intensity of all eight strips for three laser shots at each DC bias setting and laser flux. Each image was scaled according to the laser energy of each shot. For the pulsed experiments, a ~500 ps flat-top HV pulse was applied to each strip, each with different delay settings. Repeated reflections, from the infinite impedance at the end of each half-strip and the impedance mismatch at the input, broadened the voltage pulse to >1 ns full width half maximum and a peak voltage

of ~–900 V on the strip. In addition to the voltage pulse, a +200 V static bias was applied, so that the peak voltage ~–700 V. Average sensitivity in the pulsed experiments was calculated as the average intensity over an area of interest in a selected strip for five laser shots at each time-delayed setting.

IV. DISCUSSION

In the simulations, the effect of increasing the laser power was approximated by increasing the mean number of primary electrons. A true comparison to the experimental data would require knowledge of the quantum efficiency of the MCP for 200-nm photons, which is not available in literature. However, given the large number of photons/channel per laser pulse for even the lower fluxes we conclude that the quantum efficiency must be <0.1% for the MCP to detect no indication of saturation at these fluxes. Lacking knowledge of MCP glass quantum efficiency, comparison of simulations to data is based on the relative increase in primary electron number, assuming that the mean number of primary electrons scales linearly with the laser flux. Thus, we performed simulations with the mean number of primary electrons δ_0 varying between 1 and 5000.

The simulation results comparing raw electron numbers versus voltage are shown in Figure 1. The simulations exhibit strong gain saturation at high voltages when the mean number of primary electrons is between 100 and 1000. It is clear that there is a rather sharp cutoff at ~10^5 electrons, where the gain curve exhibits a plateau.

Experimental data and simulations results have been plotted together in Figure 2. All data are scaled to have the same value at –550 V, because this voltage is well above the unit gain threshold of the MCP (400–500 V for these MCPs). A quantitative comparison

is not possible since we do not know the number of electrons being extracted from the MCP, but the qualitative agreement is promising. The experimental data show appreciable saturation at higher voltages for photon fluxes >7 × 10^4 photons/channel, but saturation is absent at lower fluxes. There is, however, a fairly steep drop-off in the sensitivity for voltages below ~–550 V; this drop-off is not present for higher photon fluxes. It is also clear that the gain versus voltage sensitivity changes somewhat with laser power. As the laser flux is increased the gain becomes slightly less dependent on voltage, changing from about a $G \sim V^{11}$ dependence to more nearly a $G \sim V^{9}$ dependence before the onset of saturation. The simulations exhibit a similar trend, changing from $G \sim V^{11}$ at a mean of 1 primary electron, to $G \sim V^{8.5}$ in the linear (nonsaturated) range at a mean of 5000 primary electrons. This implies that this decrease in the gain sensitivity may arise from a 'weak' saturation resulting from high electron numbers present in the channel at a given time. It is interesting to note that this effect is seen even if the MCP is not necessarily operating at a very high gain.

It is of great importance for the fielding of the 8-frame camera on the ZR machine to know the effective dynamic range of the camera in pulsed mode. To test the dynamic range of the camera, the timing delay between the laser pulse and the voltage pulse was fixed to obtain the maximum signal from the strip in question. With the delay fixed, the laser flux was varied, ideally until the camera response was no longer linear. However, as Figure 3 shows, the camera response remains linear throughout the range of laser powers used. This result is somewhat surprising given that under static voltage bias conditions the MCP saturated at much lower laser power at similar voltage. The apparent discrepancy is likely due to two factors: 1) the difference between static and pulsed

behavior—the peak voltage in the pulse is only achieved for a relatively short time; and 2) timing uncertainties in the experimental system.

We approximated the dynamic range experiments using the simulation code by starting a cascade at the time on the voltage pulse that produced the highest eventual yield of output electrons. The number of output electrons was then tallied. To simulate the effect of increasing the laser power, the number of primary electrons was increased until the relationship of output electrons to primary electrons was no longer linear. The simulation results are shown in Figure 4. The response is linear up to δ_0~500. Thus, with the HV pulse and DC offset used, the simulations imply the camera should have a dynamic range from 10^2 to 10^3. Experimental data indicate it may in fact be somewhat greater, but the aforementioned difficulties with interpreting the data make it uncertain.

ACKNOWLEDGMENTS

This manuscript has been authored by National Security Technologies, LLC, under Contract No. DE-AC52-06NA25946 with the U.S. Department of Energy. The United States Government retains and the publisher, by accepting the article for publication, acknowledges that the United States Government retains a non-exclusive, paid-up, irrevocable, world-wide license to publish or reproduce the published form of this manuscript, or allow others to do so, for United States Government purposes.

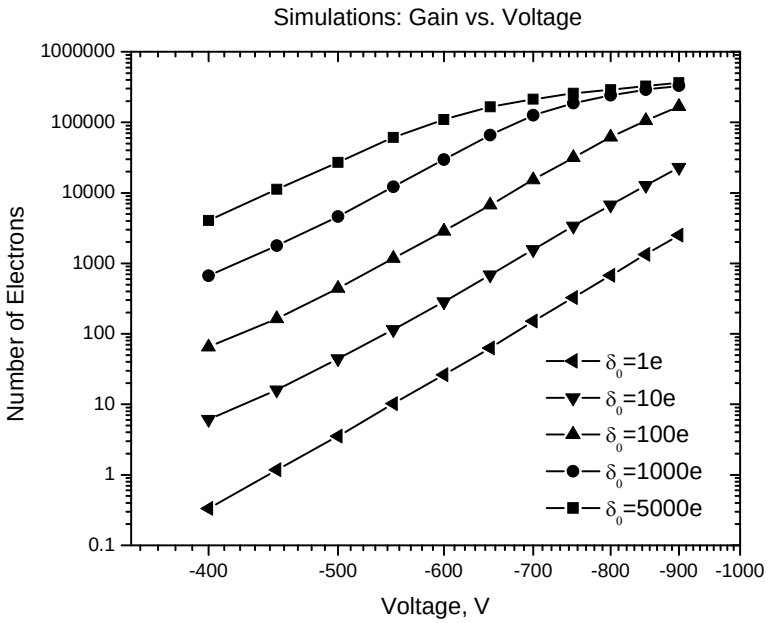

Figure 1. Simulations of electrons out vs. voltage for static voltage bias. Number of mean primary electrons is indicated. The simulations exhibit clear gain saturation for electron numbers greater than 10^5.

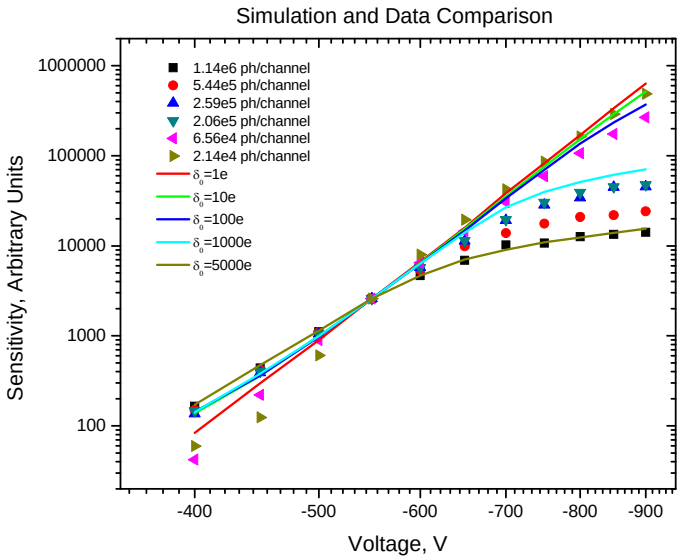

Figure 2. Comparison of simulations and experimental data. All data and simulations scaled to be equal for –550 V.

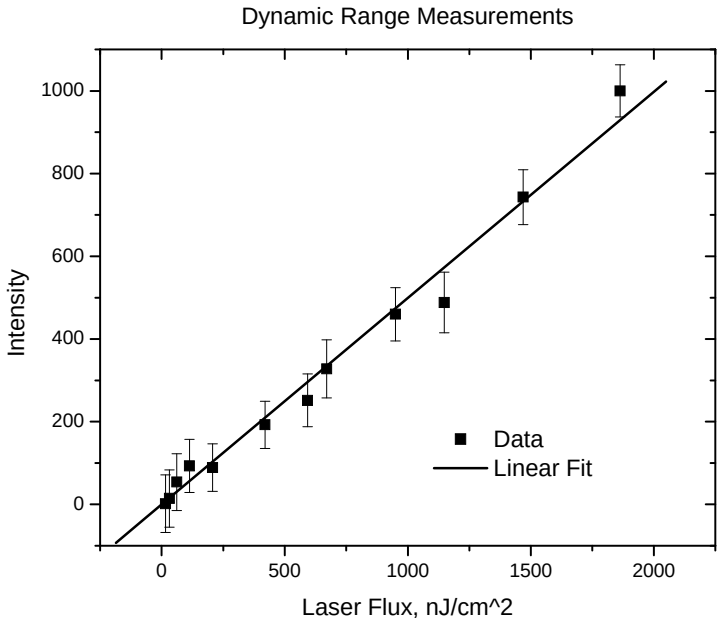

Figure 3. Data from pulsed dynamic range experiments. The detector response remains linear for the entire range of laser powers investigated.

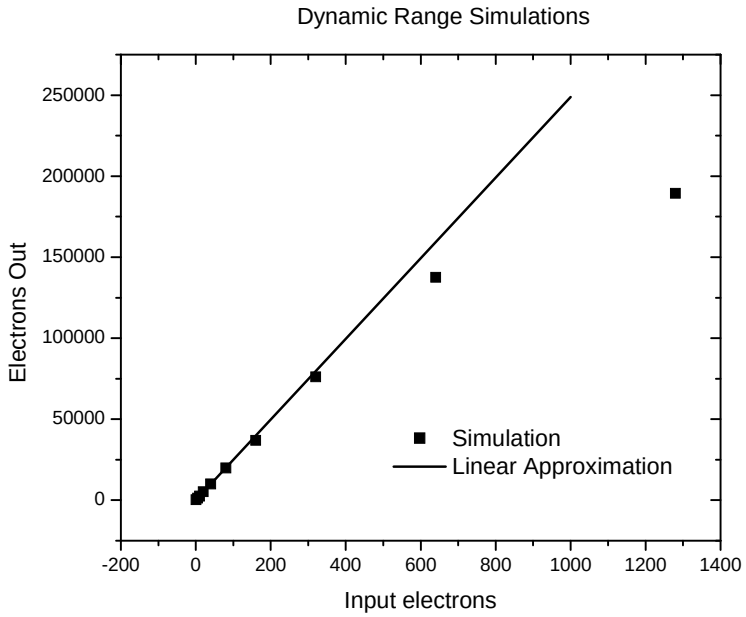

Figure 4. Results of simulations of pulsed detector dynamic range. The simulations indicate a dynamic range of 10^2 to 10^3.

[1] B. Jones, C. Deeney, A. Pirela, C Meyer, D. Petmecky, P. Gard, R Clark, and J. Davis, Rev. Sci. Instrum. **75**, 4029 (2004).

[2] M. Wu, C. A. Kruschwitz, Dane V. Morgan, and Jiaming Morgan, Rev. Sci. Instrum. submitted**,** (2008).

[3] A. J. Guest, Acta Electronica **14**, 79 (1971).

[4] M. Ito and K. Oba, IEEE Trans. Nucl. Sci. **NS-31**, 408 (1984).

[5] Y. S. Choi and J. M. Kim, IEEE Trans. Elec. Dev. **47**, 1293 (2000).

[6] G. J. Price and G.W. Fraser, Nucl. Instrum. Methods Phys. Res. A **474**, 188 (2001).

[7] E Gatti, K. Oba, and P. Rehak, IEEE Trans. Nucl. Sci. **NS-30**, 461 (1983).

[8] J. Cazaux, J. Appl. Phys. **85**, 1137 (1999).

[9] J. L. Wiza, Nucl. Instrum. Methods **162**, 587 (1979).

[10] J. Cazaux, Eur. Phys. J. AP **15**, 167 (2001).